Correcting for vital effects in coral carbonate using triple oxygen isotopes

D. Bajnai, S. Klipsch, A.J. Davies, J. Raddatz, E. Gischler, A. Rüggeberg, A. Pack, D. Herwartz

Supplementary Information

The Supplementary Information includes:

- Supplementary discussion on systematic errors
- Tables S-1 to S-3
- Figures S-1 to S-7
- Supplementary Information References

Evaluation of potential systematic errors associated with the chosen reference frame

The calculated vital effects slope values are sensitive to the reference frame used, and only the correct reference frame will provide accurate empirical triple oxygen isotope slope values for the vital effects. This is not problematic for the concept of "seeing through the vital effects" but may affect the interpretation with respect to the underlying process (*i.e.*, the second part of the discussion: "looking at the vital effect"). The θ_{coral} values presented in the main text are obtained using the theoretical Guo and Zhou (2019) aragonite equilibrium calibration. There are several published equilibrium lines, and because there is no consensus on which one is the most accurate, our choice is arbitrary.

The mean θ_{coral} value obtained using the Hayles *et al.* (2018) equilibrium aragonite calibrations is 0.530 ± 0.001 (within a range of 0.528 to 0.532), within error identical to the value derived using the Guo and Zhou (2019) calibrations of 0.529 ± 0.001 (within a range of 0.527 to 0.531). Both of these equilibrium curves are based on theory; thus, it is not surprising that they give similar results. Using the empirical aragonite α^{18}-*T* relationship of Kim *et al.* (2007) in combination with the empirical equilibrium θ–T calibration of Wostbrock *et al.* (2020) gives 0.531 ± 0.007 (within a range of 0.525 to 0.560), which is identical to the previous two θ_{coral} estimates. However, because superimposed kinetic effects on the natural aragonite samples cannot be excluded, we prefer using a theoretical calibration.

Regardless of the reference frame, the θ_{coral} values are close to the CO_2 absorption slope (ca. 0.532; see Figure S-7), indicating that CO_2 absorption is the dominating kinetic process. Only the degree of diffusion depends on which reference frame is the most accurate.

Supplementary Tables

Table S-1 Overview of the growth parameters of the coral samples in this study. Database values are interpolated from the gridded dataset of Breitkreuz *et al.* (2018). cwc = cold-water coral; wwc = warm-water coral. In brackets next to the sample names are the Sample IDs used in Davies *et al.* (2022). Sample JCB03 is from Passey *et al.* (2014).

Sample name	Type	Species	Latitude	Longitude	Depth (m)	Measured *T* (°C)	Measured $\delta^{18}O_{sw}$ (‰ VSMOW)	Database *T* (°C)	Database $\delta^{18}O_{sw}$ (‰ VSMOW)	Reference
SK-01 (LP04)	cwc	*Desmophyllum pertusum*	70.26733	22.45617	250	5.9	0.18	3.15(±1.01)	0.44(±0.44)	(Raddatz *et al.*. 2013)
SK-02 (LP03)	cwc	*Desmophyllum pertusum*	23.83535	-89	558		0.17	7.40(±1.00)	0.32(±0.32)	
SK-05 (LP-SM-U)	cwc	*Desmophyllum pertusum*	-9.82287	12.77382	374			10.17(±1.00)	0.26(±0.26)	
SK-06 (LP02)	cwc	*Desmophyllum pertusum*	51.449	-11.7527	881	9	0.4	8.92(±1.00)	0.51(±0.51)	(Raddatz *et al.*. 2013)
SK-07	cwc	*Desmophyllum pertusum*	53.51517	-14.3527	696			9.02(±1.00)	0.49(±0.49)	
SK-08 (MO01)	cwc	*Madrepora oculata*	41.28981	17.27812	573	13.5	1.16	15.14(±1.00)	1.61(±1.61)	(Schleinkofer *et al.*, 2019)
SK-09 (DD01)	cwc	*Desmophyllum dianthus*	41.28981	17.27812	573	13.5	1.16	15.14(±1.00)	1.61(±1.61)	
SK-12 (SV01)	cwc	*Solenosmilia variabilis*	-42.727	179.897	1100			4.95(±1.00)	-0.06(±-0.06)	
SK-A4	wwc	*Acropora cervicornis*	16.95725	-88.0436	6		1.2	27.24(±1.31)	0.95(±0.95)	(Gischler and Storz, 2009)
SK-A6	wwc	*Acropora* sp.	4.268056	72.93528	1	29.3	0.52	28.11(±1.14)	0.57(±0.57)	(Storz *et al.*, 2013)
SK-DS3	wwc	*Pseudodiploria strigosa*	16.95725	-88.0436	6		1.2	27.24(±1.31)	0.95(±0.95)	(Gischler and Storz, 2009)
SK-GeoB	cwc	*Desmophyllum pertusum*	34.99967	-7.07517	738	10.3	0.47	11.16(±1.00)	0.93(±0.93)	
SK-LostCity	cwc	*Desmophyllum pertusum*	30.12461	-42.1194	806.06	10.02	0.6	9.98(±1.00)	0.54(±0.54)	(Früh-Green *et al.*, 2017)
SK-PL7	wwc	*Porites lutea*	28.81648	48.77541	1	26		25.84(±3.51)	1.04(±1.04)	(Gischler *et al.*, 2005)
SK-Q43	wwc	*Porites lutea*	28.81648	48.77541	1	26		25.84(±3.51)	1.04(±1.04)	(Gischler *et al.*, 2005)
SK-SA5	wwc	*Siderastrea siderea*	17.38778	-87.9398	1		1.2	27.29(±1.42)	0.96(±0.96)	(Gischler and Storz, 2009)
SK-SV42	cwc	*Solenosmilia variabilis*	-44.498	-174.817	1386	3.8		3.02(±1.00)	-0.09(±-0.09)	(Endress *et al.*. 2022)
JCB03	wwc	*Porites porites*	24.83	-76.33	1	26		26.09(±2.21)	0.90(±0.90)	(Passey *et al.*, 2014)

Table S-2 Contains the results of the carbonate triple oxygen isotope analyses on a replicate level is available for download (.xlsx) from the online version of this article at http://doi.org/10.7185/geochemlet.2430

Table S-3 Contains the averaged results of the triple oxygen isotope analyses for each sample, including both the CO_2 and the acid-fractionation-corrected isotope values. This table also includes the measured and the database-derived seawater parameters, the vital effect slopes (θ_{coral}), and the vital effect-corrected temperatures ($T_{\Delta'17O}$), and respective uncertainties. A subset of this table is displayed below, showing acid fractionation-corrected isotope values. Data for sample JCB03 is based on Table 3 in Passey *et al.* (2014). A complete version of **Table S-3** showing all columns is available for download (.xlsx) from the online version of this article at http://doi.org/10.7185/geochemlet.2430

Sample name	Type	Species	Replicates	$\delta^{18}O$ (‰ VSMOW)	±1 S.D. $\delta^{18}O$ (‰ VSMOW)	$\Delta'^{17}O$ (ppm)	±1 S.D. $\Delta'^{17}O$ (ppm)	θ_{coral}
SK-01 (LP04)	cwc	*Desmophyllum pertusum*	4	30.58	0.04	-102	5	0.527
SK-02 (LP03)	cwc	*Desmophyllum pertusum*	2	29.88	0.11	-109	1	0.529
SK-05 (LP-SM-U)	cwc	*Desmophyllum pertusum*	5	30.81	0.07	-106	7	0.530
SK-06 (LP02)	cwc	*Desmophyllum pertusum*	2	32.72	0.02	-109	4	0.531
SK-07	cwc	*Desmophyllum pertusum*	3	30.68	0.11	-108	2	0.530
SK-08 (MO01)	cwc	*Madrepora oculata*	2	30.36	0.00	-103	9	0.530
SK-09 (DD01)	cwc	*Desmophyllum dianthus*	4	30.61	0.17	-93	5	0.528
SK-12 (SV01)	cwc	*Solenosmilia variabilis*	2	31.61	0.06	-108	3	0.529
SK-A4	wwc	*Acropora cervicornis*	5	26.93	0.16	-84	9	0.528
SK-A6	wwc	*Acropora sp.*	6	27.50	0.13	-88	4	0.530
SK-DS3	wwc	*Pseudodiploria strigosa*	5	26.38	0.06	-89	8	0.529
SK-GeoB	cwc	*Desmophyllum pertusum*	4	32.23	0.13	-109	10	0.531
SK-LostCity	cwc	*Desmophyllum pertusum*	4	33.20	0.11	-100	4	0.529
SK-PL7	wwc	*Porites lutea*	7	27.63	0.16	-91	5	0.530
SK-Q43	wwc	*Porites lutea*	7	27.30	0.11	-85	8	0.528
SK-SA5	wwc	*Siderastrea siderea*	4	26.81	0.15	-91	4	0.530
SK-SV42	cwc	*Solenosmilia variabilis*	4	32.70	0.10	-117	5	0.531
JCB03	wwc	*Porites porites*	3	28.62	0.60	-92	13	0.530

Tables S-1 to S-3 as CSV files, as well as the Python codes used to create the manuscript figures, are deposited at GitHub (https://github.com/davidbajnai/coral-triple-o) and Zenodo (https://doi.org/10.5281/zenodo.11277153).

Supplementary Figures

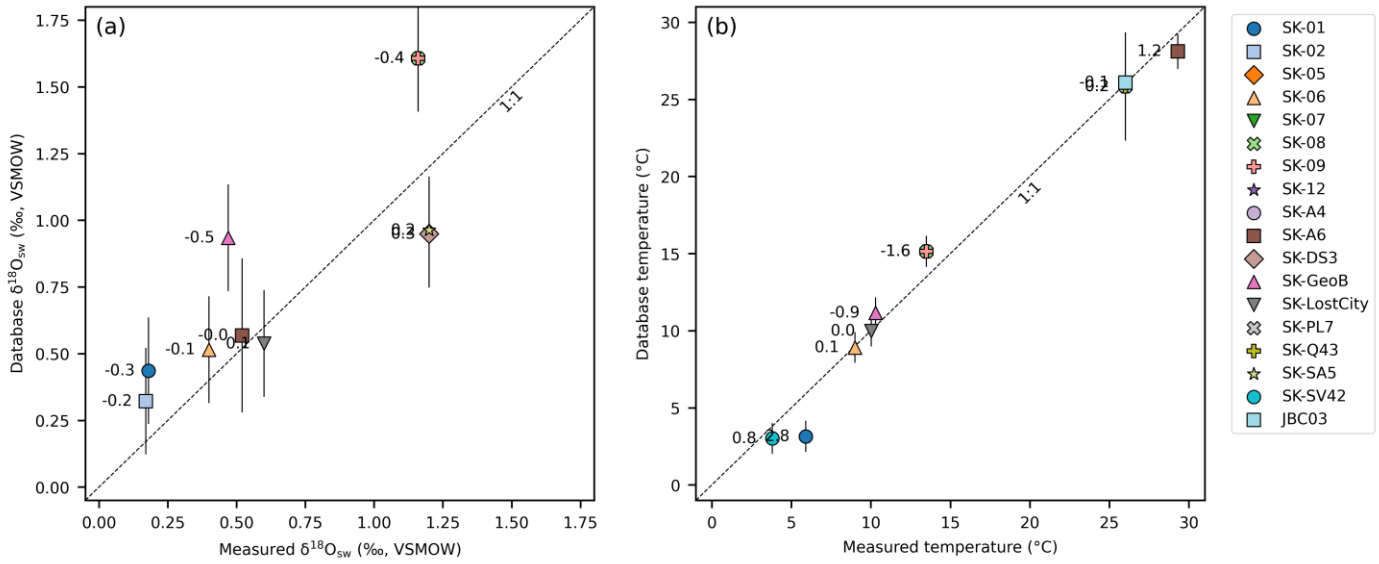

Figure S-1 Comparison of the seawater parameters measured in-situ and retrieved from the gridded database of Breitkreuz *et al.* (2018). **(a)** Seawater $\delta^{18}O$ values. **(b)** Seawater temperatures. The displayed values indicate the difference between the measured and database values.

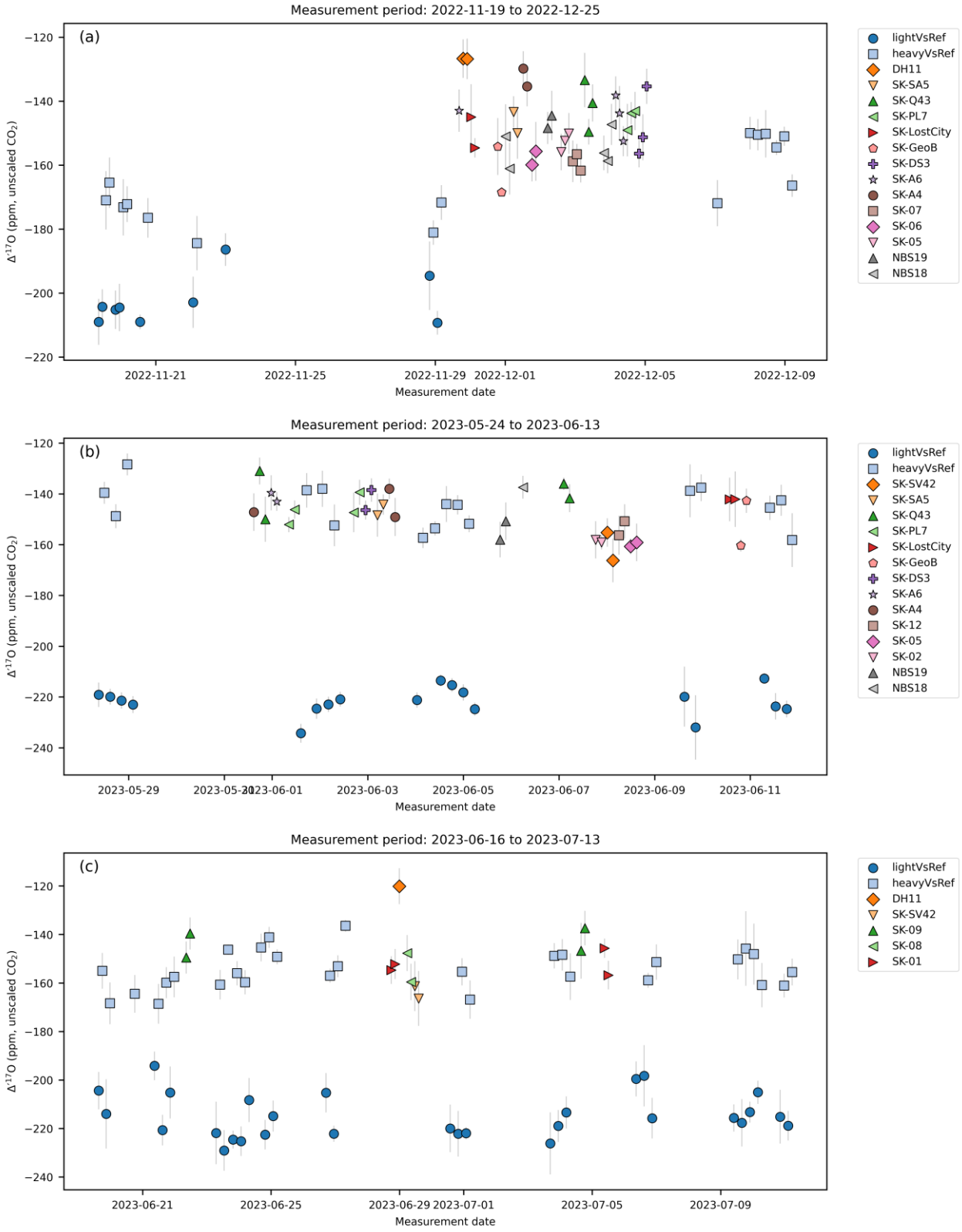

Figure S-2 (a, b, c) Unscaled Δ'^{17}O values from the three measurement periods.

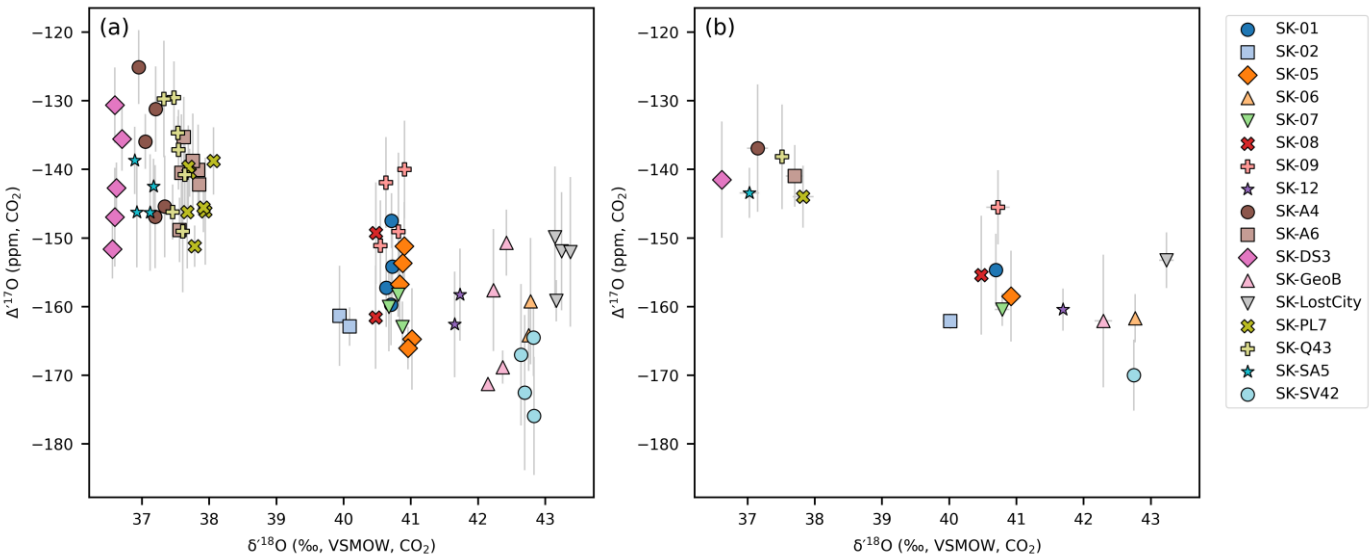

Figure S-3 (a) All replicate measurements from the three measurement periods. **(b)** The replicate measurements averaged.

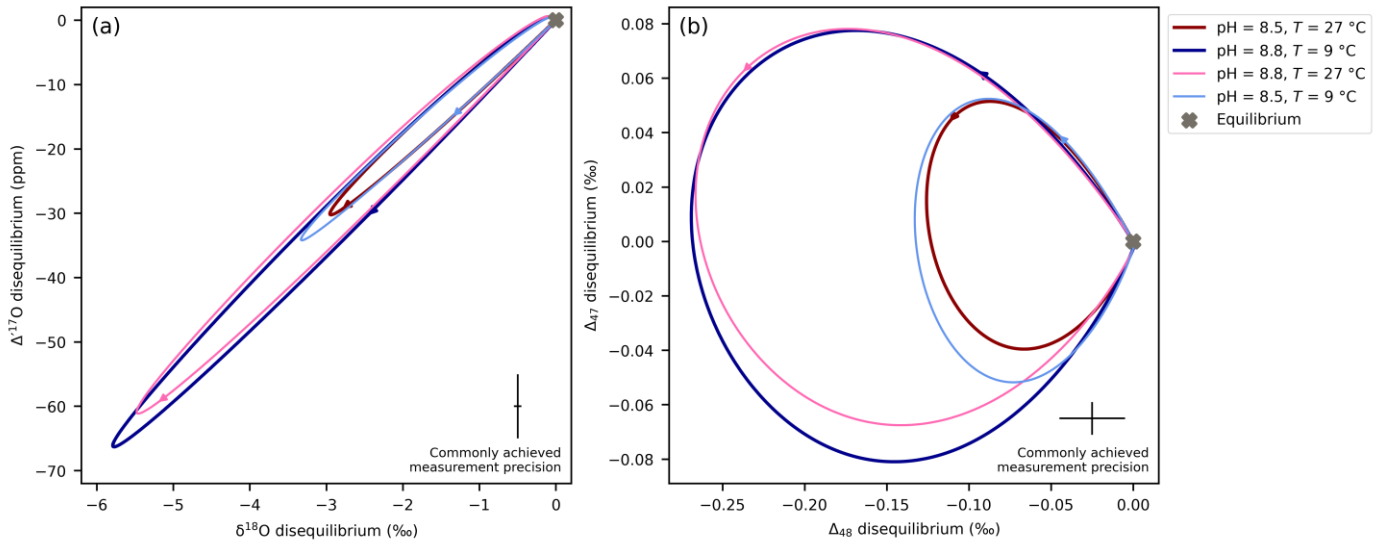

Figure S-4 CO_2 absorption simulations for **(a)** triple oxygen isotopes and **(b)** clumped isotopes. The simulations were made using the IsoDIC model (Guo, 2020). Imitating the internal calcification environment of the cold- and warm-water corals (Bajnai *et al.*, 2020; Davies *et al.*, 2022), the modelled calcification environment consisted of an aqueous solution ([DIC] = 2 mM, $\delta^{13}C_{DIC}$ = 0, and pH = 8.8 for cold-water corals and pH = 8.5 for warm-water corals), which was exposed to a CO_2-containing atmosphere (pCO_2 = 1100 ppm and $\delta^{13}C_{CO2}$ = -15‰). The temperature of the modelled calcification environment corresponded to the mean growth temperatures of the cold- and warm-water corals, *i.e.*, 9 °C and 27 °C, respectively. The initial oxygen isotope compositions of both the DIC and CO_2 were assumed to be in isotopic equilibrium with the water ($\delta^{18}O_{H2O}$ = 0‰ VSMOW) at the respective temperatures. The arrowheads show the t = 900 s of the model simulations. The lighter-coloured dashed lines show the effect of a change in the pH (*i.e.*, from 8.8 to 8.5 for the cold-water corals and from 8.5 to 8.8 for the warm-water corals).

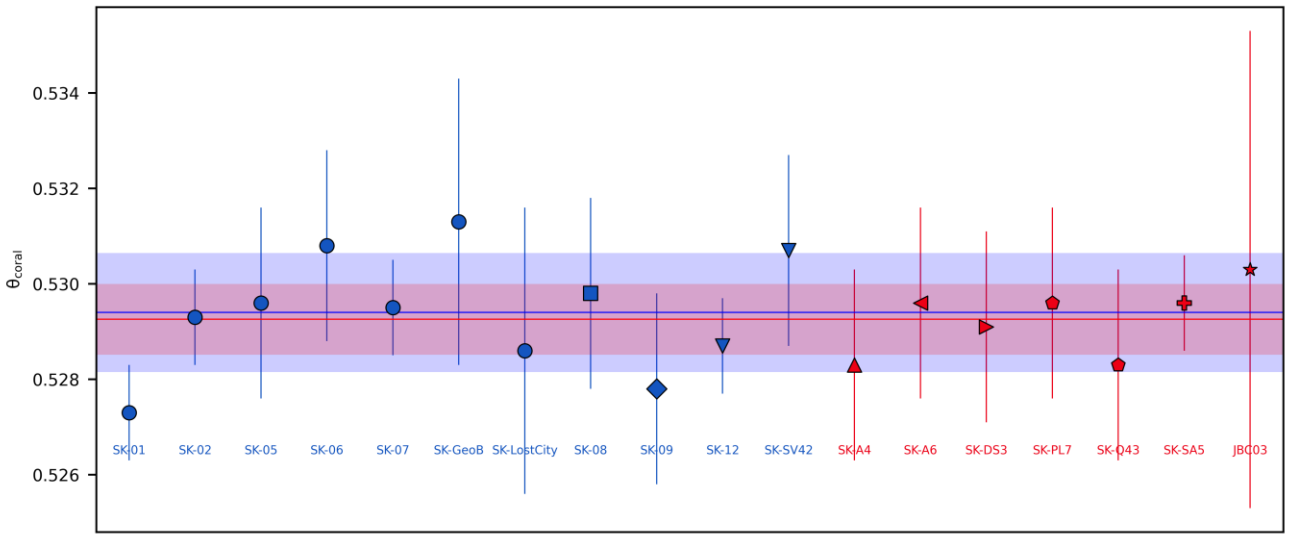

Figure S-5 This figure illustrates that there is no resolvable difference in θ_{coral} among species or between cold-water and warm-water corals. The blue and red horizontal lines represent the average values for cold-water and warm-water corals, respectively. The shaded areas indicate the range of ±1 standard deviation for the respective θ_{coral} values. When rounding the θ_{coral} values to three decimal places, as done for the temperature calculations, the mean θ_{coral} values for both cold-water and warm-water corals will become identical. Sample JCB03 is from Passey *et al.* (2014).

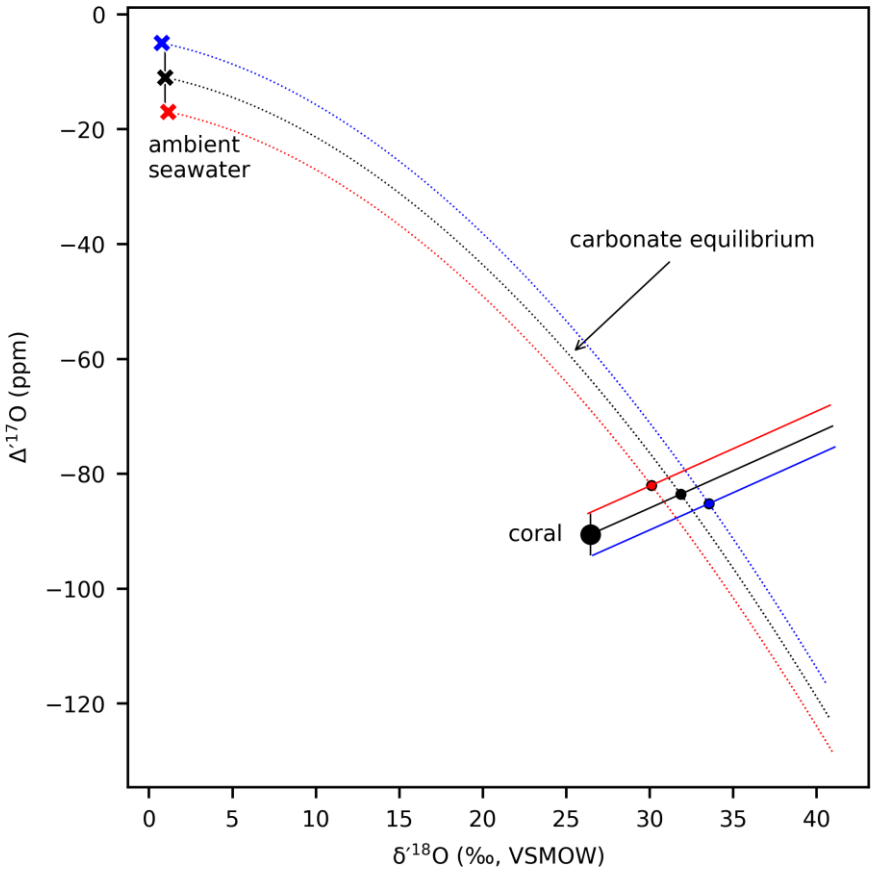

Figure S-6 This figure illustrates the full error propagation on the vital effect-corrected temperature estimates ($T_{\Delta'17O}$). The red dot shows the maximum temperature estimate, calculated using the lowest seawater $\Delta'^{17}O$ and the highest seawater $\delta^{18}O$ estimates (red cross), as well as the highest carbonate $\Delta'^{17}O$, and the lowest carbonate $\delta^{18}O$ values. The blue dot represents the minimum temperature estimate (values *vice versa*). The average $T_{\Delta'17O}$ uncertainty derived after full error propagation is ±10 °C. However, in the main text, we argue that the ±6 ppm uncertainty of the waters' $\Delta'^{17}O$ values is likely overestimated. When considering only the coral triple oxygen isotope measurement errors, the $T_{\Delta'17O}$ uncertainty reduces to ±5 °C.

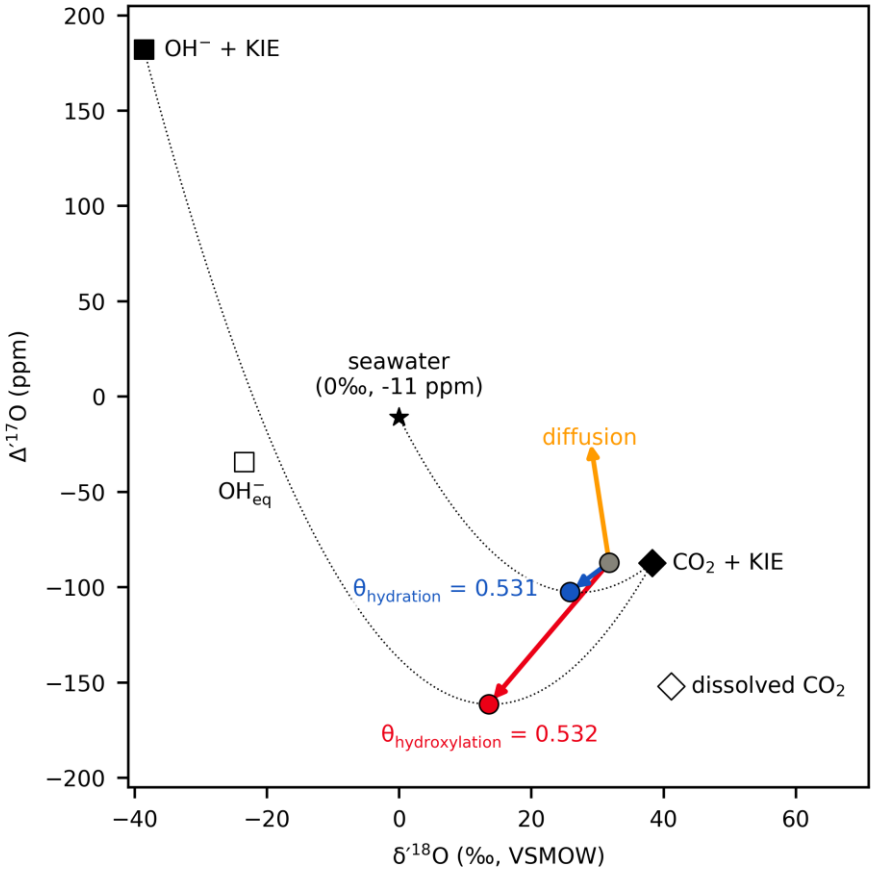

Figure S-7 Estimates for the CO_2 hydration and hydroxylation slopes in triple oxygen isotope space. The triple oxygen isotope composition of the hydration and hydroxylation endmember carbonates is calculated from a mass balance between the reacting species (Bajnai *et al.*, 2024). The equilibrium and kinetic fractionations between the hydroxide ion and ambient water are determined based on the studies by Bajnai and Herwartz (2021), Bajnai *et al.* (2024), and Zeebe (2020). The isotope composition of the dissolved CO_2 in equilibrium with ambient water is estimated from Guo and Zhou (2019). The kinetic isotope effect superimposed on the dissolved CO_2 is -3‰ in $\delta^{18}O$ (estimated from Christensen *et al.* (2021)) and assumes a θ of 0.506 for diffusion. The position of the equilibrium carbonate is calculated using the theoretical aragonite calibration of Guo and Zhou (2019). The $\theta_{hydration}$ and $\theta_{hydroxylation}$ are calculated for 25 °C, but they do not show any significant temperature dependence.

Supplementary Information References

Bajnai, D., Cao, X., Klipsch, S., Pack, A., Herwartz, D. (2024) Triple oxygen isotope systematics of CO_2 hydroxylation. *Chemical Geology* 654, 122059. https://doi.org/10.1016/j.chemgeo.2024.122059

Bajnai, D., Guo, W., Spötl, C., Coplen, T.B., Methner, K., Löffler, N., Krsnik, E., Gischler, E., Hansen, M., Henkel, D., Price, G.D., Raddatz, J., Scholz, D., Fiebig, J. (2020) Dual clumped isotope thermometry resolves kinetic biases in carbonate formation temperatures. *Nature Communications* 11, 4005. https://doi.org/10.1038/s41467-020-17501-0

Bajnai, D., Herwartz, D. (2021) Kinetic oxygen isotope fractionation between water and aqueous OH^- during hydroxylation of CO_2. *ACS Earth and Space Chemistry* 5, 3375–3384. https://doi.org/10.1021/acsearthspacechem.1c00194

Breitkreuz, C., Paul, A., Kurahashi-Nakamura, T., Losch, M., Schulz, M. (2018) A dynamical reconstruction of the global monthly mean oxygen isotopic composition of seawater. *Journal of Geophysical Research: Oceans* 123, 7206–7219. https://doi.org/10.1029/2018JC014300

Christensen, J.N., Watkins, J.M., Devriendt, L.S., DePaolo, D.J., Conrad, M.E., Voltolini, M., Yang, W., Dong, W. (2021) Isotopic fractionation accompanying CO2 hydroxylation and carbonate precipitation from high pH waters at The Cedars, California, USA. *Geochimica et Cosmochimica Acta* 301, 91–115. https://doi.org/10.1016/j.gca.2021.01.003

Davies, A.J., Guo, W., Bernecker, M., Tagliavento, M., Raddatz, J., Gischler, E., Flögel, S., Fiebig, J. (2022) Dual clumped isotope thermometry of coral carbonate. Geochimica et Cosmochimica Acta 338, 66–78. https://doi.org/10.1016/j.gca.2022.10.015

Endress, S., Schleinkofer, N., Schmidt, A., Tracey, D., Frank, N., Raddatz, J. (2022) The cold-water coral Solenosmilia variabilis as a paleoceanographic archive for the reconstruction of intermediate water mass temperature variability on the Brazilian continental margin. *Frontiers in Marine Science* 9, 909407. https://doi.org/10.3389/fmars.2022.909407

Früh-Green, G.L., Orcutt, B.N., Green, S.L., Cotterill, C., Morgan, S., Akizawa, N., Bayrakci, G., Behrmann, J.-H., Boschi, C., Brazelton, W.J., Cannat, M., Dunkel, K.G., Escartin, J., Harris, M., Herrero-Bervera, E., Hesse, K., John, B.E., Lang, S.Q., Lilley, M.D., Liu, H.-Q., Mayhew, L.E., McCaig, A.M., Menez, B., Morono, Y., Quéméneur, M., Rouméjon, S., Sandaruwan, A., Schrenk, M.O., Schwarzenbach, E.M., Twing, K.I., Weis, D., Whattam, S.A., Williams, M., Zhao, R. (2017) Central Sites. In: Früh-Green, G.L., Orcutt, B.N., Green, S.L., Cotterill, C., Expedition 357 Scientists (Eds.) *Proceedings of the International Ocean Discovery Program*, Volume 357: Atlantis Massif Serpentinization and Life https://doi.org/10.14379/iodp.proc.357.2017

Gischler, E., Lomando, A.J., Alhazeem, S.H., Fiebig, J., Eisenhauer, A., Oschmann, W. (2005) Coral climate proxy data from a marginal reef area, Kuwait, northern Arabian–Persian Gulf. *Palaeogeography, Palaeoclimatology, Palaeoecology* 228, 86–95. https://doi.org/10.1016/j.palaeo.2005.03.052

Gischler, E., Storz, D. (2009) High-resolution windows into Holocene climate using proxy data from Belize corals (Central America). *Palaeobiodiversity and Palaeoenvironments* 89, 211–221. https://doi.org/10.1007/s12549-009-0011-7

Guo, W. (2020) Kinetic clumped isotope fractionation in the DIC-H_2O-CO_2 system: Patterns, controls, and implications. *Geochimica et Cosmochimica Acta* 268, 230–257. https://doi.org/10.1016/j.gca.2019.07.055

Guo, W., Zhou, C. (2019) Triple oxygen isotope fractionation in the DIC-H_2O-CO_2 system: A numerical framework and its implications. *Geochimica et Cosmochimica Acta* 246, 541–564. https://doi.org/10.1016/j.gca.2018.11.018

Hayles, J., Gao, C., Cao, X., Liu, Y., Bao, H. (2018) Theoretical calibration of the triple oxygen isotope thermometer. *Geochimica et Cosmochimica Acta* 235, 237–245. https://doi.org/10.1016/j.gca.2018.05.032

Kim, S.-T., Mucci, A., Taylor, B.E. (2007) Phosphoric acid fractionation factors for calcite and aragonite between 25 and 75 °C: Revisited. *Chemical Geology* 246, 135–146. https://doi.org/10.1016/j.chemgeo.2007.08.005

Passey, B.H., Hu, H., Ji, H., Montanari, S., Li, S., Henkes, G.A., Levin, N.E. (2014) Triple oxygen isotopes in biogenic and sedimentary carbonates. *Geochimica et Cosmochimica Acta* 141, 1–25. https://doi.org/10.1016/j.gca.2014.06.006

Raddatz, J., Liebetrau, V., Rüggeberg, A., Hathorne, E., Krabbenhöft, A., Eisenhauer, A., Böhm, F., Vollstaedt, H., Fietzke, J., López Correa, M., Freiwald, A., Dullo, W.C. (2013) Stable Sr-isotope, Sr/Ca, Mg/Ca, Li/Ca and Mg/Li ratios in the scleractinian cold-water coral Lophelia pertusa. *Chemical Geology* 352, 143–152. https://doi.org/10.1016/j.chemgeo.2013.06.013

Schleinkofer, N., Raddatz, J., Freiwald, A., Evans, D., Beuck, L., Rüggeberg, A., Liebetrau, V. (2019) Environmental and biological controls on Na/Ca ratios in scleractinian cold-water corals. *Biogeosciences* 16, 3565–3582. https://doi.org/10.5194/bg-16-3565-2019

Storz, D., Gischler, E., Fiebig, J., Eisenhauer, A., Garbe-Schonberg, D. (2013) Evaluation of oxygen isotope and Sr/Ca ratios from a Maldivian scleractinian coral for reconstruction of climate variability in the northwestern Indian Ocean. *Palaios* 28, 42–55. https://doi.org/10.2110/palo.2012.p12-034r

Wostbrock, J.A.G., Brand, U., Coplen, T.B., Swart, P.K., Carlson, S.J., Brearley, A.J., Sharp, Z.D. (2020) Calibration of carbonate-water triple oxygen isotope fractionation: Seeing through diagenesis in ancient carbonates. *Geochimica et Cosmochimica Acta* 288, 369–388. https://doi.org/10.1016/j.gca.2020.07.045

Zeebe, R.E. (2020) Oxygen isotope fractionation between water and the aqueous hydroxide ion. *Geochimica et Cosmochimica Acta* 289, 182–195. https://doi.org/10.1016/j.gca.2020.08.025